Appl Phys B (2011) 102: 509–514
DOI 10.1007/s00340-011-4428-0

Applied Physics B
Lasers and Optics

Thermal analysis and efficient high power continuous-wave and mode-locked thin disk laser operation of Yb-doped sesquioxides

R. Peters · C. Kränkel · S.T. Fredrich-Thornton · K. Beil · K. Petermann · G. Huber · O.H. Heckl · C.R.E. Baer · C.J. Saraceno · T. Südmeyer · U. Keller

Received: 29 June 2010 / Published online: 15 February 2011

Abstract We report on thermal conductivity analysis and thin disk laser power scaling of Yb:Lu_2O_3, Yb:Sc_2O_3, and Yb:$LuScO_3$. Using a volume Bragg-grating stabilized pump diode we have obtained cw output powers up to 301 W with optical-to-optical efficiencies of up to 73%. In mode-locked operation of an Yb:Lu_2O_3 thin disk laser 141 W of average output power with 738 fs pulses and an optical-to-optical efficiency of 40% were achieved.

1 Introduction

Currently multi-kilowatt continuous-wave (cw) thin disk lasers based on the gain material Yb:YAG have become commercially successful thanks to their high efficiency and good beam quality. For example in welding applications in the automotive industry these lasers allowed for narrow and deep weld seams (similar to electron beam welding) and for highly productive remote processing [1].

Yb-doped sesquioxides have been recognized as a potentially more efficient gain material than Yb:YAG [2–4]. A high mechanical strength in combination with excellent thermal properties and high absorption cross sections make them ideally suited for the thin disk laser geometry [5]. They are also very suitable for high average power femtosecond ultrafast sources due to their larger emission bandwidths in comparison to Yb:YAG [6, 7]. However, the growth of sesquioxide crystals with their high melting points around 2400°C is challenging (see Table 1) which results in a poor crystal quality and optical-to-optical efficiency of less than 50% in previous experiments [8, 9]. During the last years these difficulties have been overcome with the heat exchanger method (HEM) for the growth of high quality, large scale sesquioxide crystals [10]. These improved Yb-doped sesquioxides achieved higher efficiencies than any other gain material in the thin disk laser geometry: first continuous-wave (cw) and mode-locked thin disk laser experiments were based on Yb:Lu_2O_3 (Yb:LuO) as the gain material, followed by the successful cw-laser operation with Yb:Sc_2O_3 (Yb:ScO) crystals, [11–13]. More recently, the disordered $LuScO_3$ (LuScO) [14] was successfully introduced as a host material for the Yb-ion [15]. The broad spectra resulting from the disordered lattice has supported the shortest pulses in a mode-locked thin disk oscillator with 227 fs duration so far [16].

In this work we present the results on power scaling of Yb-doped sesquioxide thin disk based on high quality HEM-grown Yb:LuO, Yb:ScO, and Yb:LuScO crystals. With all three materials, the cw output power could be increased by nearly an order of magnitude to more than 250 W and the cw mode-locked average output power to more than 140 W, which have been to the best of our knowledge the highest average power from any cw and cw mode-locked sesquioxide laser reported so far.

2 Thermal conductivity

In most host materials the thermal conductivity of the laser crystal drops significantly if the doping concentration of the

R. Peters (✉) · C. Kränkel · S.T. Fredrich-Thornton · K. Beil · K. Petermann · G. Huber
Institute of Laser-Physics, University of Hamburg, Luruper Chaussee 149, 22761 Hamburg, Germany
e-mail: rpeters@physnet.uni-hamburg.de
Fax: +49-40-89985199

C. Kränkel · O.H. Heckl · C.R.E. Baer · C.J. Saraceno · T. Südmeyer · U. Keller
Department of Physics, Institute of Quantum Electronics, ETH Zurich, Wolfgang-Pauli-Strasse 16, 8093 Zurich, Switzerland

Table 1 Relevant spectroscopic and thermal properties at room temperature of the different Yb-doped sesquioxides in comparison to Yb:YAG [3, 9, 29]

Properties		Unit	$LuScO_3$	Sc_2O_3	Lu_2O_3	YAG
Thermal conductivity	undoped	W/(m K)	3.6	17.3	12.6	11
	doped[a]		3.5	7	12	7
Cation density (for 1 at.%)		10^{20} cm^{-3}	3.10	3.36	2.85	1.38
Pump wavelength		nm	975.7	975.1	976.0	940
Absorption cross section		10^{-20} cm^2	3.3	4.4	3.1	0.83
Absorption bandwidth (FWHM)		nm	2.4	2.1	2.9	12.5
Melting temperature		°C	2370	2430	2450	1940

[a]The considered doping concentration is $8 \cdot 10^{20}$ cm^{-3}, which is a reasonable value for use in thin disk lasers

active ion is increased (see Table 1). This effect is caused by the different atomic weights of the substituted cation and the doping ion. In insulators like YAG or the sesquioxides where heat transport takes place mainly by propagating phonons, these phonons are scattered at the mass defects leading to decreasing thermal conductivity with increasing doping level [17]. Due to the larger mass difference ($m_{Yb} = 173.5$ g/mol) this decrease is strongest in Yb:ScO ($m_{Sc} = 44.96$ g/mol) and weakest in Yb:LuO ($m_{Lu} = 174.97$ g/mol) [18].

Motivated by further power scaling the dependence of the thermal conductivity on the doping concentration was investigated by applying the temperature-wave analysis method [19]. For that goal a "mobile 1" device for thermal diffusivity measurements from ai-Phase (Japan) has been used to examine a number of undoped and Yb-doped sesquioxide samples with doping concentrations between 0% and 100% with respect to the cation sites. All samples had a thickness of roughly 0.5 mm. The thermal conductivity was finally calculated by multiplication with the heat capacity and the density of the different materials. Considering these results as well as values from the literature [3] a theoretical model due to Klemens [17, 20] was applied to describe the progression of the thermal conductivity in dependence of the Yb-concentration. In this model the decrease of the thermal conductivity is attributed to phonon scattering at the doping ions which are treated as point defects. With the temperature T the resulting fit function is

$$\kappa(c) = \kappa_m(c)\sqrt{\frac{\chi \cdot T}{\varepsilon(c)}} \cdot \arctan\sqrt{\frac{\varepsilon(c)}{\chi \cdot T}},$$

where $\kappa(c)$ describes the thermal conductivity in dependence of the doping concentration c, and

$$\kappa_m(c) = (1 - c) \cdot \kappa_0 + c \cdot \kappa_{100}$$

the arithmetic average of the thermal conductivity of the undoped and 100%-doped crystal. $\varepsilon(c)$ a term describing the phonon scattering due to mass defects, which can be directly calculated from the ionic masses of the Yb-ion and substituted cation by

$$\varepsilon(c) = \sum_i \frac{c_i (M_i - M)^2}{M^2} \quad \text{with } M = \sum_i c_i M_i.$$

The parameter χ, representing the product of different intrinsic constants, e.g. phonon velocity and lattice modes, is used as the only fit parameter. Details on this method can be found in [17, 21].

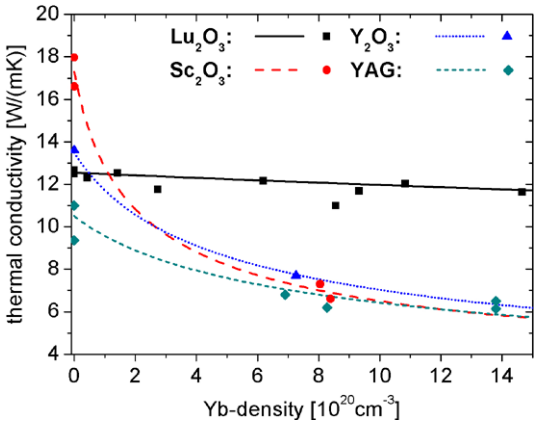

Fig. 1 Measured (*symbols*) and fitted (*lines*) thermal conductivity of the different Yb:sesquioxides and Yb:YAG for Yb-concentrations between 0 and $15 \cdot 10^{20}$ cm^{-3} (corresponding to Yb(10.9 at.%):YAG, Yb(5.3 at.%):LuO, Yb(4.5 at.%)ScO, and Yb(5.6 at.%)YO)

Figure 1 presents the results of the measurements and the fit in the doping range relevant for laser experiments. For all materials a good agreement between the measured and calculated values is observed over the whole doping range. Due to the reasons discussed above, the strongest decrease in thermal conductivity is found in Yb:ScO, for which a drop from 17.3 W/(m K) in the undoped host to about 7 W/(m K) at an Yb-density of $8 \cdot 10^{20}$ cm^{-3} (~2.4 at.% Yb) can be seen. Starting from about 14 W/(m K) and 11 W/(m K) a similar decrease can be observed for Yb:Y_2O_3 (Yb:YO)

and Yb:YAG, respectively, leading to comparable values of 7 W/(m K) at an Yb-density of $8 \cdot 10^{20}$ cm^{-3}. In contrast to Yb:ScO, Yb:YO, and Yb:YAG the thermal conductivity of Yb:LuO is only slightly reduced from 12.6 W/(m K) to 12 W/(m K) at the same Yb-concentration, which can be attributed to the very small mass difference between the Lu and Yb-ion of only 1.1%. Due to the high intrinsic distortion of the lattice in the disordered LuScO a relatively low thermal conductivity of 3.6 W/(m K) has been measured. As expected, increasing the Yb-doping concentration to $8 \cdot 10^{20}$ cm^{-3} only slightly decreases the thermal conductivity to 3.5 W/(m K).

In conclusion, due to an efficient heat removal from the active media, the very high thermal conductivity of Yb:LuO at high doping levels leads to significant advantages for power scaling purposes. Nevertheless, it should be noted that also Yb:ScO and Yb:YO show excellent thermal properties being at least comparable to those of Yb:YAG.

3 Experimental laser setup

The laser experiments were performed with different 150 µm to 400 µm thick Yb:LuO, Yb:ScO, and Yb:LuScO disks with Yb-doping concentrations between 2 at.% and 5 at.% corresponding to concentrations between $5.8 \cdot 10^{20}$ cm^{-3} and $1.5 \cdot 10^{21}$ cm^{-3}, respectively. The crystal diameter was 5 mm for the Yb:LuO samples and 6.5 mm for the Yb:ScO as well as Yb:LuScO samples. Each disk was soldered onto a water-cooled metal heat sink. As pump source, a volume Bragg-grating (VBG) stabilized [22] pump diode from DILAS Diodenlaser GmbH with about 400 W of output power [23] was used. This diode was developed to match the zero-phonon-line absorption of Yb:LuO at 976 nm, showing only a very low wavelength shift with output power and temperature due to the VBG-stabilization. Hence, with its central emission wavelength of 976.2 nm, it did not perfectly match the absorption of the other two examined materials, which show an optimum absorption at slightly shorter wavelengths (see Fig. 2). Nevertheless the fraction of absorbed pump power in all examined crystals is well above 95% for all output coupler transmissions and the corresponding inversion levels in the applied thin disk laser pump module with 24 pump light passes through the gain medium. At the maximum pump current the diode generates more than 410 W of output power within a FWHM bandwidth of less than 0.6 nm.

In all experiments a simple I-type resonator was formed by the backside of the disk, which was HR-coated for the spectral range of pump- and laser wavelengths, and the output coupling mirror with 500 mm radius of curvature. For output coupling mirrors with transmissions between 1.2% and 4.2% for the laser wavelength have been used. The short

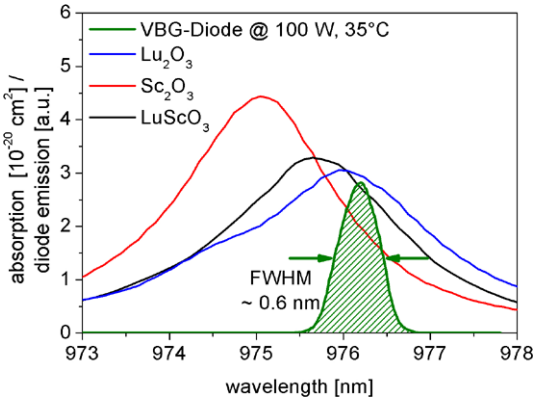

Fig. 2 Absorption cross sections at the zero-phonon-line for the three different Yb-doped sesquioxide materials in comparison to the diode emission spectrum at a diode output power of 100 W. The 0.6 nm broad emission peak of the VBG-stabilized diode perfectly fits into the absorption peak of Yb:LuO

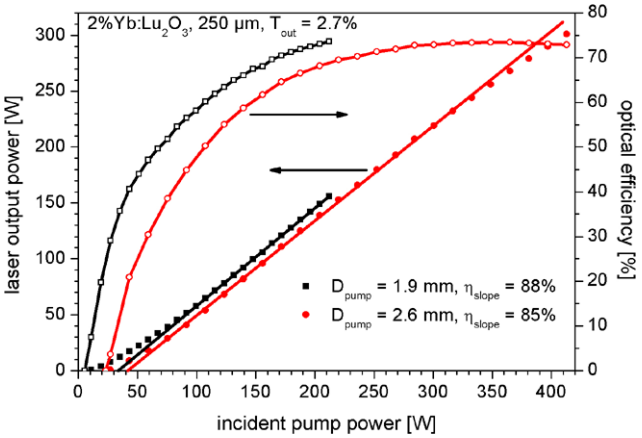

Fig. 3 Laser characteristics of a 250 µm Yb(2 at.%):LuO disk for different pump spot diameters and the experimentally verified optimum outcoupling rate of 2.7%. Due to the comparably small disk diameter of only 5 mm the disk could not be pumped with the largest available pump spot diameter of 4 mm

resonator length between 75 mm and 90 mm led to multimode operation. This enabled highest efficiencies and simple alignment, allowing for a reliable comparison of the different materials. By changing the lens in the pump collimation optics, the pump spot diameter could be varied between 1.9 mm, 2.6 mm, and 4 mm.

4 CW results and discussion

Figure 3 shows the best results obtained with Yb:LuO disks at a pump spot diameter of 2.6 mm for the optimum outcoupling rate of $T_{\text{out}} = 2.7\%$. In this case the largest adjustable pump spot size of 4 mm could not be used, because the available Yb:LuO disks were limited by the small disk diameter of 5 mm and possible damage in the edge regions,

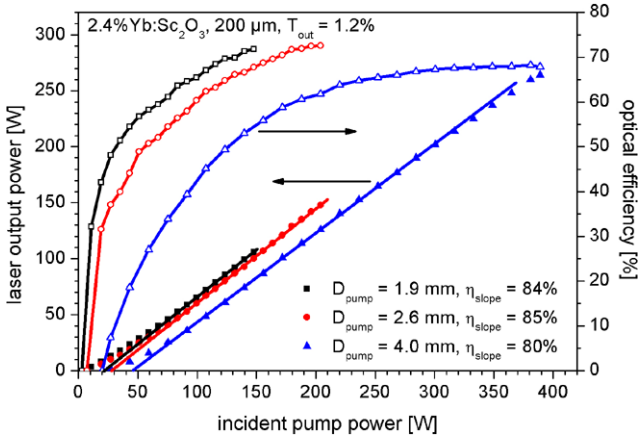

Fig. 4 Laser characteristics of a 200 µm Yb(2.4 at.%):ScO disk for different pump spot diameters and the experimentally verified optimum outcoupling rate of 1.2%

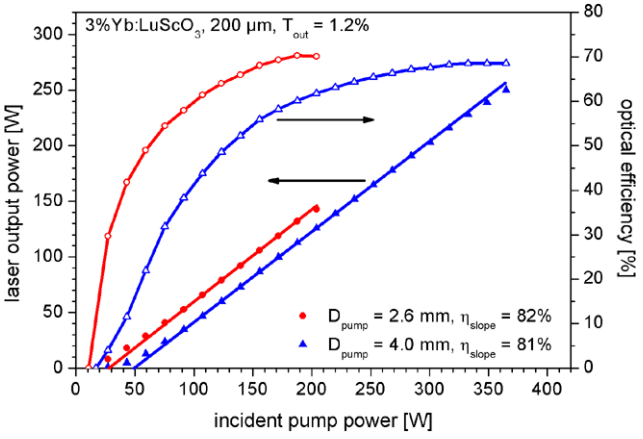

Fig. 5 Laser characteristics of a 200 µm Yb(3 at.%):LuScO disk for different pump spot diameters and the experimentally verified optimum outcoupling rate of 1.2%. During the experiments the crystal was damaged, before data for a pump spot diameter of 1.9 mm could be recorded

which were for technical reasons not soldered to the heat sink. The 250-µm thick disk with an Yb-doping concentration of 2 at.% generates 301 W of output power at a center wavelength of 1034 nm under 413 W of incident pump power, which corresponds to an optical-to-optical efficiency of 73%. At pump powers of more than 370 W, corresponding to a pump power density of 7 kW/cm^2, a slight decrease in efficiency can be seen, which is probably caused by a thermal rollover. It has to be noted that this disk was mounted with an indium-tin solder onto a copper heat sink, whereas commercial thin disk lasers at these power levels are often glued to diamond heat sinks or at least mounted with the more suitable gold-tin solder [24]. Decreasing the pump spot diameter to 1.9 mm led to an even higher optical-to-optical efficiency of 74% and a record high slope efficiency of 88% (see Fig. 3).

In contrast to the Yb:LuO samples, the larger aperture of the Yb:ScO and Yb:LuScO disks allowed for the largest available pump spot diameter of 4 mm. Both materials showed the best performance and slope efficiencies above 80% with an output coupler transmission of 1.2%, underlining the extremely low internal losses of the HEM-grown crystals. With an Yb(2.4 at.%):ScO disk of 200 µm thickness, maximum output powers of 264 W, 148 W, and 106 W for 4.0 mm, 2.6 mm, and 1.9 mm pump spot diameter, respectively, were measured with optical-to-optical efficiencies around 70% (see Fig. 4). The pump power was limited to 380 W for this material because damage was observed with other Yb:ScO samples at comparable pump power intensities.

Figure 5 presents the results achieved with a 3 at.% doped Yb:LuScO disk of 200 µm thickness. Despite its low thermal conductivity mentioned previously in this work, a high output power of 250 W was obtained at 365 W incident pump power in a 4 mm pump spot, corresponding to a pump power density of 2.9 kW/cm^2. The optical-to-optical efficiency was 69%. For a pump spot diameter of 2.6 mm the efficiency could be increased to slightly above 70%, but due to the higher pump power density of 3.8 kW/cm^2 the crystal was damaged at 204 W of pump power, which was probably caused by mechanical stress due to grain boundaries in the pump spot area as reported in [16]. For that reason, no result with a 1.9 mm pump spot is presented in Fig. 5. The parameters of the laser setups which delivered the highest output power for each material are summarized in Table 2.

5 Mode-locking results

With a 250-µm thick Yb(2 at.%)LuO-disk, a semiconductor saturable absorber mirror (SESAM) [25] ($F_{\mathrm{sat}} = 61$ µJ/cm^2, $\Delta R = 0.5\%$, non-saturable losses $<0.1\%$), and a set of 9 GTI-type dispersive mirrors (total GDD ≈ -9900 fs^2), mode-locking experiments were performed. The pump spot was 2.6 mm in diameter and the output coupler mirror had a transmission of 9%. We obtained stable mode-locked operation with an average output power of 141 W and an optical-to-optical efficiency of 40.4% at a repetition rate of 60 MHz. This has been to the best of our knowledge the highest average output power reported from a mode-locked laser oscillator. The ideal soliton pulses [26] had a duration of 738 fs (FWHM) and an energy of 2.4 µJ. A more detailed discussion of the experimental setup and the achieved results is given in [27].

6 Conclusion and outlook

In conclusion, we have discussed the thermal properties of Yb-doped sesquioxide crystals. Applying a theoretical

Table 2 Comparison of the laser parameters for the maximum output power and the corresponding results for each of the three examined materials

	Unit	$LuScO_3$	Sc_2O_3	Lu_2O_3
Laser wavelength	nm	1041	1042	1034
Outcoupling transmission	%	1.2	1.2	2.7
Disk thickness	µm	200	200	250
Doping concentration	%	3	2.4	2
Pump spot diameter	mm	4	4	2.6
Pump power	W	365	380	413
Output power	W	250	264	301
Optical-to-optical efficiency	%	69	70	73
Slope efficiency	%	81	80	85
Pump power density	kW/cm^2	2.9	3.0	7.8

model to measured values, the progression of the thermal conductivity in dependence of the Yb-concentration was described, documenting the great potential of these materials as high power solid state lasers.

Using a VBG-stabilized pump diode we could demonstrate power scaling of the sesquioxides Yb:LuO, Yb:ScO, and their stoichiometric mixture Yb:LuScO. Output powers above 250 W could be obtained for all three materials with more than 70% optical-to-optical efficiency. In particular, with Yb:LuO a record high slope efficiency of 88% and 301 W of output power in multi-mode operation as well as 141 W of average power with 40% optical-to-optical efficiency and 738 fs pulses in mode-locked operation were realized. These results exceed previously achieved results with Yb:YAG in terms of efficiency and output power [28], demonstrating the potential for further scaling of the output parameters of femtosecond thin disk lasers. Promising in this respect is also the achieved power scaling of the mixed crystal Yb:LuScO to 250 W at 69% optical-to-optical efficiency. In initial mode-locking experiments with this material, pulses as short as 227 fs were obtained, which are the shortest pulses from any thin disk laser reported so far [16].

All materials appear promising for a further scaling of the output power to the kW-level by applying disks with a larger diameter mounted on state-of-the-art diamond heat sinks using volume Bragg-grating stabilized pump diodes.

Acknowledgement We acknowledge financial support by the German Federal Ministry of Education and Research (BMBF, contract number 13N8382), the Joachim Herz Stiftung in Hamburg, and the Swiss National Science Foundation (SNF) in Zurich, Switzerland. Furthermore, we thank Birgit Weichelt from the Institut für Strahlwerkzeuge (IFSW) in Stuttgart for mounting several of the disks used in these experiments.

References

1. A. Giesen, J. Speiser, IEEE J. Sel. Top. Quantum Electron. **13**, 598 (2007)
2. L. Fornasiero, E. Mix, V. Peters, K. Petermann, G. Huber, Cryst. Res. Technol. **34**, 255 (1999)
3. K. Petermann, G. Huber, L. Fornasiero, S. Kuch, E. Mix, V. Peters, S.A. Basun, J. Lumin. **87–89**, 973 (2000)
4. K. Petermann, L. Fornasiero, E. Mix, V. Peters, Opt. Mater. **19**, 67 (2002)
5. A. Giesen, H. Hügel, A. Voss, K. Wittig, U. Brauch, H. Opower, Appl. Phys. B **58**, 365 (1994)
6. T. Südmeyer, C. Kränkel, C.R.E. Baer, O.H. Heckl, C.J. Saraceno, M. Golling, R. Peters, K. Petermann, G. Huber, U. Keller, Appl. Phys. B **97**, 281 (2009)
7. M. Tokurakawa, A. Shirakawa, K. Ueda, H. Yagi, M. Noriyuki, T. Yanagitani, A.A. Kaminskii, Opt. Express **17**, 3353 (2009)
8. K. Petermann, D. Fagundes-Peters, J. Johannsen, M. Mond, V. Peters, J.J. Romero, S. Kutovoi, J. Speiser, A. Giesen, J. Cryst. Growth **275**, 135 (2005)
9. P. Klopp, V. Petrov, U. Griebner, K. Petermann, V. Peters, G. Erbert, Opt. Lett. **29**, 391 (2004)
10. R. Peters, C. Kränkel, K. Petermann, G. Huber, J. Cryst. Growth **310**, 1934 (2008)
11. R. Peters, C. Kränkel, K. Petermann, G. Huber, Opt. Express **15**, 7075 (2007)
12. C.R.E. Baer, C. Kränkel, C.J. Saraceno, O.H. Heckl, M. Golling, T. Südmeyer, R. Peters, K. Petermann, G. Huber, U. Keller, Opt. Lett. **34**, 2823 (2009)
13. R. Peters, K. Beil, C. Kränkel, K. Schenk, K. Petermann, G. Huber, in *Conference on Lasers and Electro-Optics (Europe)*, Munich, Germany (2009), paper CA9.1
14. K.S. Bagdasarov, A.A. Kaminskii, A.M. Kevorkov, L. Li, A.M. Prokhorov, T.A. Tevosyan, S.E. Sarkisov, Sov. Phys. Dokl. **20**, 681 (1975)
15. R. Peters, K. Petermann, G. Huber, in *Advanced Solid-State Photonics (ASSP)*, Denver, USA (2009), paper MC4
16. C.R.E. Baer, C. Kränkel, O.H. Heckl, M. Golling, T. Südmeyer, R. Peters, K. Petermann, G. Huber, U. Keller, Opt. Express **17**, 10725 (2009)
17. P.G. Klemens, Phys. Rev. **119**, 507 (1960)
18. T.B. Coplen, Pure Appl. Chem. **73**, 667 (2001)
19. J. Morikawa, T. Hashimoto, Jpn. J. Appl. Phys. **37**, L1484 (1998)
20. R. Gaumé, B. Viana, D. Vivien, J.P. Roger, D. Fournier, Appl. Phys. Lett. **83**, 1355 (2003)
21. H. Marquardt, S. Ganschow, F.R. Schilling, Phys. Chem. Miner. **36**, 107 (2008)
22. G.B. Venus, A. Sevian, V.I. Smirnov, L.B. Glebov, in *Conference on High-Power Diode Laser Technology and Applications III*, San Jose, CA, ed. by M.S. Zediker (Springer, Berlin, 2005), pp. 166–176
23. B. Köhler, T. Brandt, M. Haag, J. Biesenbach, in *Photonics West*, San José, USA (2009), p. 719810

24. M. Larionov, PhD thesis, 2009
25. U. Keller, K.J. Weingarten, F.X. Kärtner, D. Kopf, B. Braun, I.D. Jung, R. Fluck, C. Hönninger, N. Matuschek, J. Aus der Au, IEEE J. Sel. Top. Quantum Electron. **2**, 435 (1996)
26. F.X. Kärtner, U. Keller, Opt. Lett. **20**, 16 (1995)
27. C.R.E. Baer, C. Kränkel, C.J. Saraceno, O.H. Heckl, M. Golling, R. Peters, K. Petermann, T. Südmeyer, G. Huber, U. Keller, Opt. Lett. **35**, 2302 (2010)
28. J. Mende, E. Schmid, J. Speiser, G. Spindler, A. Giesen, in *Solid State Lasers XVIII: Technology and Devices*, ed. by W.A. Clarkson, N. Hodgson, R.K. Shori, Proceedings of the SPIE, vol. 7193 (Springer, Berlin, 2009), p. 71931
29. D. Fagundes-Peters, N. Martynyuk, K. Lünstedt, V. Peters, K. Petermann, G. Huber, S. Basun, V. Laguta, A. Hofstaetter, J. Lumin. **125**, 238 (2007)